

# Cytotoxic and Catalytic Features of New Asymmetric Copper(II) Schiff-Base Complexes

Zahra Saedi<sup>a,\*</sup>, Mahmoud Roushani<sup>a</sup>, Elham Hoveizi<sup>b,c</sup>, Mohammad Hadian<sup>a</sup>

<sup>a</sup>Department of Chemistry, Faculty of Science, Ilam University, Ilam, Iran

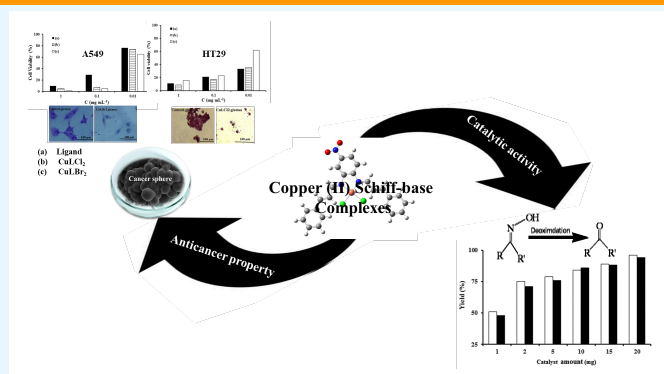
<sup>b</sup>Department of Biology, Faculty of Science, Shahid Chamran University of Ahvaz, Ahvaz, Iran

<sup>c</sup>Stem Cells and Transgenic Technology Research Center (STTRC), Shahid Chamran University of Ahvaz, Ahvaz, Iran

Received: January 11, 2024; Accepted: February 11, 2024

**Cite This:** *Inorg. Chem. Res.* **2023**, *7*, 42-50. DOI: 10.22036/j10.22036.2024.435220.1157

**Abstract:** The bidentate Schiff-base ligand, *N,N'*-bis(*E*)-3-phenylallylidene)-4-nitro-1,2-phenylenediamine, [L], was synthesized and characterized along with its Cu(II) complexes, CuLX<sub>2</sub> (where X = Cl and Br). The characterization involved elemental analysis, <sup>1</sup>H NMR, <sup>13</sup>C NMR, FT-IR, and UV-Vis spectroscopy, as well as thermal and conductivity studies. The elemental analyses of these complexes were consistent with the stoichiometry of the type CuLX<sub>2</sub>. The confirmation of their stabilization and their slight electrolytic nature is reinforced by their low molar conductivity. Furthermore, the alterations in both the location and shape of the peaks in the UV-Vis and FT-IR spectra of the complexes, relative to those of the free ligand, serve as additional evidence supporting the formation of Schiff-base complexes. Also, cathodic and anodic shifted in the potential's peaks of complexes compared to free ligand approve formation of compounds. Catalytic activity of these complexes in the room temperature deoxygenation using sodium periodate were studied. Obtained aldehydes and ketones as single products in excellent yields confirm catalytic activity of these complexes. Lastly, *in vitro* cytotoxic features of all samples studied against A549 and HT29 cancer cell lines and the outcomes exhibited excellent cytotoxic potential of synthesized complexes.



**Keywords:** Schiff-base, Catalyst, Copper(II), Cytotoxic, Cancer cell line

## 1. INTRODUCTION

Schiff-base ligands containing the azomethine group (RCH=NR', where R and R' represent alkyl and/or aryl substituents) are often referred to as 'privileged ligands' due to their typical formation through the condensation reaction between active C=O carbonyl compounds and primary amines.<sup>1,2</sup> These ligands have the capability to coordinate with a wide range of metal ions and effectively stabilize them in diverse oxidation states.<sup>3</sup> Some applications of Schiff-bases can be mentioned as colored materials, catalytic agents, intermediates of inorganic synthesis, and as stabilizers of polymers.<sup>4-9</sup> Most of Schiff-bases have demonstrated a wide spectrum of biological activities, encompassing antitumor, antibacterial, fungicidal, and anticarcinogenic properties.<sup>10-12</sup> Metal complexes formed by Schiff-bases in conjunction with heterocyclic compounds are also utilized for their potential as pharmaceutical agents, owing to the presence of multifunctional groups.<sup>13-18</sup> Copper(II) complexes have exhibited remarkable catalytic activity in various oxidation reactions<sup>19-22</sup> and have also been significant interest as antitumor agents. For tumor

angiogenesis processes copper as a cofactor is essential. Additionally, copper has the capability to induce the generation of reactive oxygen species (ROS) within human cells, as indicated by studies.<sup>23-26</sup> These studies, which involve investigations into the biological properties of Cu(II) complexes such as DNA binding, DNA cleavage, anticancer, and antimicrobial activities, have been extensively documented in the literature.<sup>27-31</sup> Cu(II) complexes are regarded as a promising alternative to *cis*-platin complexes in the area of anticancer activity due to their biocompatibility and their significant roles within biological systems.<sup>32,33</sup> For instance, they have the ability to accumulate within cancerous cells owing to the selective permeability of cell membranes to copper compounds.<sup>34,35</sup> Moreover, copper(II) complexes have found widespread application in metal-mediated DNA cleavage processes for the generation of activated oxygen species.<sup>36-39</sup>

In this study, we present the synthesis, characterization, and catalytic performance evaluation of two copper(II) Schiff-base complexes in the conversion of various oximes using sodium periodate. As well, the

electrochemical and thermal behaviors of all compounds were investigated. Additionally, anticancer activities of these complexes were evaluated against A549 and HT29 cancerous cell lines.

## 2. EXPERIMENTAL

### Materials and methods

*Trans*-Cinnamaldehyde, 4-nitro-1,2-phenylenediamine, copper(II) salts, sodium periodate, solvents, giemsa's azure eosin methylene blue solution (Giemsa), and other chemicals were obtained from suppliers such as Aldrich and Merck Chemicals and were employed without prior purification. 3-(4,5-Dimethyl-2-thiazolyl)-2,5-diphenyl-2*H*-tetrazolium bromide (MTT) was obtained from Sigma company. Cancer cell lines (A549 and HT29) was prepared from Iran Pasteur Institute, Tehran, Iran. Using CDCl<sub>3</sub> as the solvent and TMS as the internal standard with a BRUKER 250 MHz spectrometer, <sup>1</sup>H and <sup>13</sup>C NMR spectra were recorded. With KBr pills as the sample preparation method and Perkin Elmer version 10.01.00 FT-IR spectrometer, Infrared (IR) spectra of all compounds were measured at 4000-400 cm<sup>-1</sup> wavenumber range. Thermogravimetric analyses (TGA) were carried out with a PL-1500 TGA apparatus under N<sub>2</sub> atmosphere. The electrochemical studies utilized in a normal three-electrode cell setup, an Ag/AgCl (saturated KCl) reference electrode, a platinum electrode as the counter electrode, and a glassy carbon electrode as the working electrode. Cyclic voltammograms were conducted using a μ-AUTOLAB electrochemical system type III equipped with a FRA2 board computer-controlled Potentiostat/Galvanostat (Eco-Chemie, Switzerland). A Vario EL III CHNS system used for elemental analyses studies. Electronic spectra ranging from 200 to 1000 nm in DMF were collected using a Perkin Elmer Lambda 45 model spectrophotometer. Metrohm-712 conductometer applied to conductivity measurement experiments at room temperature in solutions of DMF and DMSO (both at a concentration of 1.0×10<sup>-3</sup> M). Cytotoxic surveys completed with spectrophotometric plate reader Expert 96, Asys Hitch, Ec Austria. Morphological investigations were done *via* reversed fluorescent microscope (Olympus, Japan).

### Synthetic producers

***N,N'*-bis(*E*)-3-phenylallylidene)-4-nitro-1,2-phenylenediamine (L).** 10 mL Ethanolic solution of *trans*-cinnamaldehyde (2 mmol, 0.132 g) gradually added to 10 mL ethanolic solution of 4-nitro-1,2-phenylenediamine (1 mmol, 0.153 g) under severe stirring for 6 h at room temperature. After cooling for 4 h in a refrigerator, a yellow solid product was filtered off, washed three times with ethanol (3×10 mL), and finally vacuum-dried. For purification of ligand, the solid product was recrystallized from ethanol.

**C<sub>24</sub>H<sub>19</sub>N<sub>3</sub>O<sub>2</sub> (L):** Yellow color; Yield: 73%; m.p. (°C): 175. FT-IR (KBr, cm<sup>-1</sup>): 3414 (w), 3324 (w), 3055 (m), 2860 (m), 1629 (s), 1583 (s), 1495 (s), 1333 (s), 1307 (s), 1150 (m), 1093 (w), 996 (w), 820 (w), 749 (m), 731 (m). <sup>1</sup>H NMR (CDCl<sub>3</sub>, ppm): 8.4 (bs, 2H), 7.07-8.00 (m, 13H), 5.01-6.70 (d, 4H). <sup>13</sup>C NMR (CDCl<sub>3</sub>, ppm): 161.20, 148.64, 145.30, 138.70, 135.49, 135.32, 129.96, 128.98, 128.04, 127.67, 124.17, 113.07, 112.87.

**Copper(II) complexes.** In the synthesis of copper(II) complexes, the following procedure was employed: anhydrous copper halide salts (1 mmol, CuCl<sub>2</sub> and CuBr<sub>2</sub>) were dissolved in 5 mL of ethanol under vigorous stirring. Subsequently, a solution of the ligand (1 mmol) in 25 mL of chloroform was added dropwise. After a reaction time of 5 hours, the resulting precipitate was filtered and washed with cold methanol. For additional purification, the complexes were subjected to recrystallization in a mixture of dimethylsulfoxide and methanol, followed by drying at temperatures ranging from 80 to 100 °C under vacuum conditions.

**CuLCl<sub>2</sub>:** Yield: 77%. m.p. (°C): 188.

FT-IR (KBr, cm<sup>-1</sup>): 3441 (w), 3246 (m), 3030 (w), 2854 (w), 1640 (vs), 1526 (s), 1434 (m), 1340 (s), 1123 (w), 1067 (m), 959 (m), 876 (m), 749 (m), 504 (w).

**CuLBr<sub>2</sub>:** Yield: 72%. m.p. (°C): 203 (dec.).

FT-IR (KBr, cm<sup>-1</sup>): 3420 (m), 3099 (w), 2924 (m), 2857 (m), 1634 (vs), 1524 (s), 1432 (m), 1341 (s), 1217 (w), 1068 (m), 962 (m), 881 (m), 749 (m), 503 (w).

### General deoximation procedure of oximes to carbonyl compounds catalyzed by copper(II) Schiff-base complexes

To assess the catalytic activity of CuLCl<sub>2</sub> and CuLBr<sub>2</sub>, we investigated their ability to catalyze the conversion of various oximes into the respective aldehydes or ketones at room temperature. In a 25 mL flask equipped with a magnetic stirrer bar, a solution of sodium periodate (2 mmol, 427 mg in 2 mL H<sub>2</sub>O) was added to a mixture of oxime (1 mmol) and CuLX<sub>2</sub> (0.020 g) in CH<sub>3</sub>CN (2 mL). The progress of the reactions was tracked by TLC (eluent: *n*-hexane-ethyl acetate, 7:2). After completion of the reaction, the product was extracted with CH<sub>2</sub>Cl<sub>2</sub> (3×10 mL) and desiccated over anhydrous Na<sub>2</sub>SO<sub>3</sub>. Simple filtration followed by solvent evaporation from the filtrate yielded the pure product in high isolated yields.

### Anticancer studies

The A549 and HT29 cancer cell lines were obtained from the Iran Pasteur Institute. These cell lines were cultured and sustained in DMEM/F12 medium, supplemented with 1% penicillin/streptomycin and 10% FBS, and incubated in an environment containing 5% CO<sub>2</sub> and 95% humidity. Changing the medium was done every 3 days. The cell viability and the metabolic activity of the cancer cells by using the 3-(4,5-dimethylthiazolyl-2-yl)-2,5-diphenyltetrazolium bromide (MTT) reduction assay was evaluated. The cells were plated at a density of 1×10<sup>4</sup> cells/well in 96-well plates and then incubated under standard condition for 24 and 72 hours. Subsequently, 100 μL of a 0.5 mg mL<sup>-1</sup> MTT solution was introduced to each well, and the plates were incubated at 37 °C for 4 hours. Afterward, the culture medium was removed, and the formazan crystals were solubilized in DMSO and by a microplate reader, the absorbance at 570 nm was estimated (Expert 96, Asys Hitch, Ec Austria). Morphology observation was performed as follows: the cells were initially seeded in a sterile 96-well plate and allowed to incubate for 24 hours. Subsequently, they were exposed to the ligand and copper(II) complexes for 24 hours. The cells were stained by the addition of 100 mL of a 4% Giemsa solution. Then, the plates were incubated at room temperature for 20 minutes, followed by thorough rinsing with distilled water and air-dried. In all experiments control groups were containing

untreated cells. Additionally, the DMSO concentration was restricted to 0.5% (v/v) in this study, and it demonstrated no significant impact on cell viability.

### 3. RESULTS AND DISCUSSION

#### Characterization studies

*N,N'*-bis((*E*)-3-phenylallylidene)-4-nitro-1,2-phenylenediamine (L) as a Schiff-base ligand was synthesized by the condensation between one equivalent of 4-nitro-1,2-phenylenediamine and two equivalents of aldehyde. This ligand was employed as a chelating agent to synthesize Cu(II) complexes with a general formula of  $\text{CuLX}_2$  ( $\text{X} = \text{Cl}$  and  $\text{Br}$ ) (Figure 1).

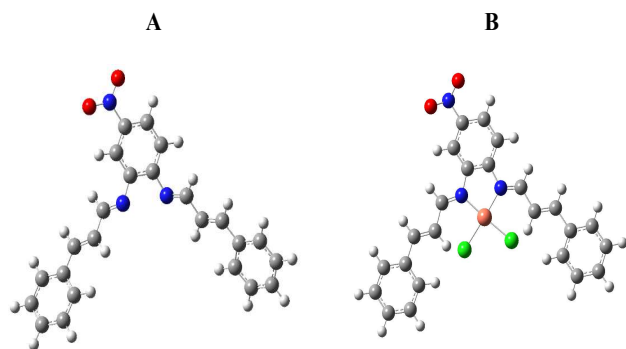


**Figure 1.** Structure of A) the Schiff-base ligand and B) Cu(II) complexes [copper (orange), nitrogen (blue), oxygen (red), halogen (green), carbon (gray) and hydrogen (white)].

The complexes exhibit insolubility in common solvents such as dichloromethane, chloroform, acetone, and alcohols; however, they display solubility in DMSO and DMF. The stoichiometry of both the ligand and its complexes was confirmed based on the elemental analyses data (Table 1). The analytical results validate the correctness of a 1:1 metal to ligand ratio for the complexes. The molar conductivity of ligand and copper complexes at  $10^{-3}$  M were measured in DMF and DMSO at room temperature and resulted data listed in Table 1. The conductivity data of copper Schiff-bases ( $<65 \text{ S cm}^2 \text{ mol}^{-1}$ , in DMF), demonstrating covalent attachment, nonionic and possibly slight electrolytic character due to molar conductance values close on  $25 \text{ S cm}^2 \text{ mol}^{-1}$  in DMSO.<sup>40-42</sup>

**Table 1.** Molecular weight, molar conductivity, and elemental analysis of the ligand and its complexes

Compound	Mol. wt.	$\lambda^{\text{M}}$ ( $\text{S cm}^2 \text{ mol}^{-1}$ )		Found (Calc.) %		
		DMF	DMSO	C	H	N
L	381.43	3.59	2.8	75.67 (75.57)	5.14 (5.03)	10.97 (11.02)
[CuLCl <sub>2</sub> ]	515.87	28.53	21.4	56.12 (55.87)	3.57 (3.71)	8.36 (8.15)
[CuLBr <sub>2</sub> ]	604.77	43.26	25.7	47.94 (47.66)	2.89 (3.17)	7.16 (6.95)

The  $^1\text{H}$  and  $^{13}\text{C}$  NMR spectra of the ligand were obtained at room temperature, with chloroform serving

as the solvent (Figure S1). The  $^1\text{H}$  NMR spectrum of the ligand shows peaks at 8.4 ppm (bs, 2H) for azomethine, 7.07-8.00 ppm (m, 13H) for aromatic and 5.01-6.70 ppm (d, 4H) for olefinic hydrogens. In the  $^{13}\text{C}$  NMR spectrum of the ligand, peaks were observed at 161.20 ppm for azomethine group and at 148.64, 145.30, 138.70, 135.49, 135.32, 129.96, 128.98, 128.04, 127.67, 124.17, 113.07, and 112.87 ppm for aromatic and olefinic carbons.

To clarify the bonding mode and the influence of the metal ion on the ligand, a comparative analysis of the FT-IR spectra was conducted for both the free ligand and its Cu(II) complexes. The assignments and comparisons are detailed in Figure S2 and Table S1. The appearance of a stretching frequency at  $1629 \text{ cm}^{-1}$  in the ligand spectrum is attributed to the C=N functional group.<sup>43-45</sup> In the copper complexes, the stretching bond exhibited a noticeable shift of approximately  $5\text{-}11 \text{ cm}^{-1}$  toward higher frequencies and appeared in the range of  $1634\text{-}1640 \text{ cm}^{-1}$ . This small shift in the IR spectra may be considered as proof of nitrogen coordination due to conjugation<sup>46</sup> and support coordination of the azomethine group with the copper ion. The peak at  $2860 \text{ cm}^{-1}$ , which is attributed to iminic C-H, exhibited a gradual shift towards lower frequencies following complexation. The ligand displayed highly intense bands at  $1583$  and  $1333 \text{ cm}^{-1}$ , which can be attributed to the asymmetric ( $\nu_{\text{asym}}$ ) and symmetric stretching ( $\nu_{\text{sym}}$ ) vibrations of the  $-\text{NO}_2$  group, respectively.<sup>47-51</sup> The absorption spectra of both the ligand and its complexes were recorded at a concentration of  $10^{-5}$  M in DMF, as shown in Figure S3. The spectral data can be found in the final column of Table S1. The ligand's spectrum displays two distinct absorption bands, located at 303 and 388 nm, which are attributed to the  $\pi\text{-}\pi^*$  transitions associated with the phenylene rings and the iminic systems, respectively.<sup>52-54</sup> As seen in Table S1, the Cu complexes corresponding to coordinated ligand show two absorption bands at 300 and 302 (first band) and 350 and 351 (second band) for  $\text{CuLBr}_2$  and  $\text{CuLCl}_2$  respectively. The second band displays blue shifted to lower wavelengths, 38 nm, that confirmed ligand coordination through nitrogen atoms. Furthermore, two complexes exhibit an absorption band as a shoulder at 365 nm, which is attributed to charge transfer from the non-bonding orbital of the nitrogen atoms to the unoccupied copper(II) d orbitals.<sup>55-57</sup> Based on absorption spectra and some reports in literatures for complexes containing bidentate Schiff-base ligands,<sup>58-60</sup> pseudo-tetrahedral geometry proposed for metal complexes. Since a four-coordinate square planar coordination complex is strongly favored for the  $d^9$  configuration, as a result of the Jahn-Teller effect, the common disorder is a flattening of the tetrahedron

along a twofold axis (Figure 1B).

Thermogravimetric analysis of both the ligand and its copper complexes (as shown in Figure S4) reveals varying thermal stability, with each undergoing decomposition at distinct temperatures. Obtained thermograms show that ligand undergoing complete decomposition, while complexes generated copper oxide as residual. As represented in the TGA plots, the decomposition processes of the complexes commenced at temperatures above 155 °C, so suggested that there are no water molecules in their structures.<sup>61</sup>

### Redox properties

A glassy carbon electrode was used for recording cyclic voltammograms (CV) of all samples ( $1.0 \times 10^{-3}$  M) in dry DMF with scan rate of  $0.1 \text{ V S}^{-1}$ . Tetrabutylammonium perchlorate (0.1 M) used as supporting electrolyte. Prior to recording the voltammograms, all solutions were deoxygenated by passing a stream of pre-purified nitrogen ( $\text{N}_2$ ) into the solution for 10 minutes. As represented in Figure 2, both the ligand and its complexes exhibit redox activity within the solvent potential window, ranging from -1.5 to 1.5 volts.

The bidentate Schiff-base ligand is reducible at negative potential -1.13 V. In positive sweep the ligand is oxidized at -0.95 V. The cathodic peak may be assigned to the reduction of the nitro group to the radical anion.<sup>62-64</sup> This electrochemical behavior could be considered as reversible processes. Copper complexes with respect to free ligand show different behaviors in their voltammograms. The copper chloride complex shows one pair anodic and cathodic peaks at 0.61 and 0.34 V correspond to Cu(II)/Cu(I) system and cathodic peak at -0.85 V correspond to Schiff-base ligand, while the copper bromide complex shows anodic peak at 1.21 V and cathodic peaks at -0.92 V correspondence to Cu(I)/Cu(II) system and ligand respectively. Cyclic voltammograms of complexes and free ligand confirm complexation.

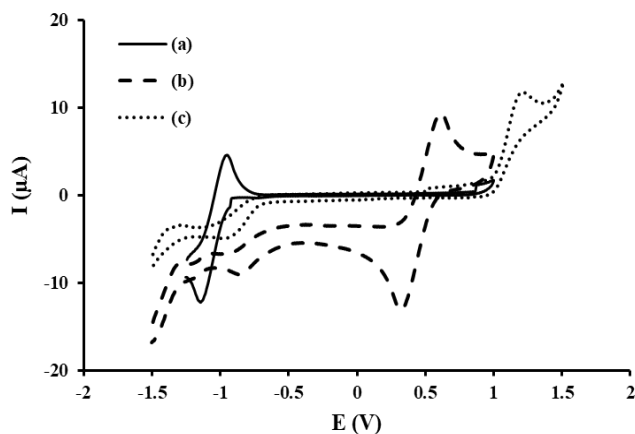
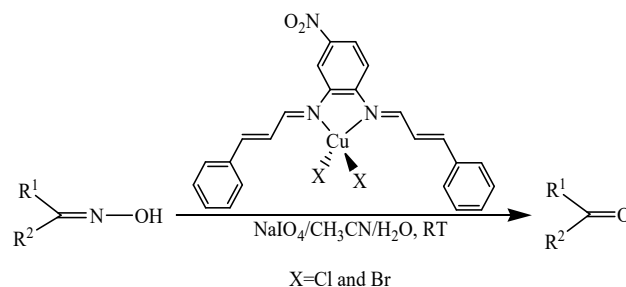


**Figure 2.** Cyclic voltammograms of a) Ligand, b)  $\text{CuLCl}_2$ , and c)  $\text{CuLBr}_2$ .

### Catalytic activity

Schiff-base transition metal complexes represent an appealing class of catalysts for a wide range of organic substrates due to their cost-effective and straightforward synthesis as well as their remarkable chemical and thermal stability.<sup>20-22,65-71</sup> Thus herein, we study the applications of copper(II) Schiff-base complexes as homogeneous catalysts in the deoxygenation of oximes using  $\text{NaIO}_4$  (Scheme 1).



**Scheme 1.** The conversion of oxime to carbonyl compounds using sodium periodate in the presence of  $\text{CuLX}_2$

To determine the optimal reaction conditions, we selected 4-chlorobenzaldehyde oxime as the model and investigated its conversion in various solvents. From a selection of solvents, including methanol, ethanol, acetone, acetonitrile (in single-phase systems), chloroform, and carbon tetrachloride (in two-phase systems using  $\text{Bu}_4\text{NBr}$  as a phase transfer catalyst) mixed with water, the 1:1 acetonitrile/water mixture was adopted as the reaction medium. This choice was based on the high solubility of the complexes in this solvent and the observed higher aldehyde yields (Table S2, entry 3).

The conversion reaction of 4-chlorobenzaldehyde oxime (1 mmol) was conducted using varying quantities of  $\text{NaIO}_4$ . It was observed that the reaction did not reach completion when less than 2 mmol of  $\text{NaIO}_4$  was used. However, employing a higher concentration (3 mmol) did not lead to an improvement in either the conversion or the selectivity of the reaction. Also, the conversion of 4-chlorobenzaldehydeoxime (1 mmol) using  $\text{NaIO}_4$  (2 mmol) in the absence and presence of Cu(II) complexes as catalysts at room temperature was examined. It was observed that the reactions were completed after 10 and 1.25 h in the absence and presence of 20 mg catalyst, respectively (Figure S5). Based on the observation, 1 mmol of substrate, 2 mmol of  $\text{NaIO}_4$ , 20 mg of catalyst and a 1:1 mixture of acetonitrile and water as reaction medium was chosen as the best combinations for deoxygenation.

To assess the broad applicability of this method, a diverse set of oximes was subjected to conversion under the optimized conditions. All the reactions occurred with high selectivity for carbonyl compounds formation (Table 2). Identities of products have been confirmed by comparison

**Table 2.** Conversion of various oximes to related carbonyl compounds by sodium periodate catalyzed by CuLCl<sub>2</sub> and CuLBr<sub>2</sub>

Entry	Substrate	Product	Yield <sup>[a]</sup> (%)		Time (min)		m.p. (°C) <sup>[b]</sup>	
			CuLCl <sub>2</sub>	CuLBr <sub>2</sub>	CuLCl <sub>2</sub>	CuLBr <sub>2</sub>	CuLCl <sub>2</sub>	CuLBr <sub>2</sub>
1	Benzophenone oxime	Benzophenone	90	85	50	50	48-50	47-51
2	Cyclohexanone oxime	Cyclohexanone	85	82	120	125	Oil	Oil
3	Cinnamaldehyde oxime	Cinnamaldehyde	91	90	80	70	Oil	Oil
4	Benzaldehyde oxime	Benzaldehyde	82	85	60	60	Oil	Oil
5	4-Dimethylaminobenzaldehyde oxime	4-Dimethylaminobenzaldehyde	97	96	60	60	72-75	72-75
6	4-Fluorobenzaldehyde oxime	4-Fluorobenzaldehyde	75	83	60	60	Oil	Oil
7	4-Chlorobenzaldehyde oxime	4-Chlorobenzaldehyde	96	94	70	75	45-47	46-50
8	4-Bromobenzaldehyde oxime	4-Bromobenzaldehyde	85	83	70	70	55-58	56-58
9	4-Methylbenzaldehyde oxime	4-Methylbenzaldehyde	96	95	50	50	Liq.	Liq.
10	4-Nitrobenzaldehyde oxime	4-Nitrobenzaldehyde	95	92	60	60	102-107	103-106
11	3-Nitrobenzaldehyde oxime	3-Nitrobenzaldehyde	90	85	50	60	57-58	56-58

Reaction condition: substrate (1 mmol), NaIO<sub>4</sub> (2 mmol) and catalyst (20 mg) in 4 mL CH<sub>3</sub>CN/H<sub>2</sub>O (1:1), room temperature.

[a] Isolated yield. [b] Melting point (m.p.) of products have been comparison with those of authentic samples.

**Table 3.** Obtained data for deoxygenation of benzophenone oxime in the presence of CuLX<sub>2</sub> (X=Cl, Br) Schiff-base complexes with other reported catalysts

Entry	Catalyst	Amount of catalyst (mol%)	Oxidant	Solvent	Time (h)	Yield (%)	Ref.
1	MCM-41	10	H <sub>2</sub> O <sub>2</sub>	(CH <sub>3</sub> ) <sub>2</sub> CO	6	67	72
2	(PhTe) <sub>2</sub> <sup>a</sup>	1	O <sub>2</sub>	-	24	93	73
3	W@PANI <sup>b</sup>	0.048	H <sub>2</sub> O <sub>2</sub>	CH <sub>3</sub> CN	24	77	74
4	(PhTe) <sub>2</sub> <sup>c</sup>	2.5	O <sub>2</sub>	-	24	93	75
5	Co(II) catalyst <sup>d</sup>	9	H <sub>2</sub> O <sub>2</sub>	CH <sub>3</sub> OH	2.5	72	76
6	(PhCH <sub>2</sub> Se) <sub>2</sub> <sup>e</sup>	2.5	H <sub>2</sub> O <sub>2</sub>	CH <sub>3</sub> CN	24	81	77
7	Fe(NO <sub>3</sub> ) <sub>3</sub> ·9H <sub>2</sub> O	2.5	O <sub>2</sub>	C <sub>6</sub> H <sub>5</sub> CH <sub>3</sub>	1.5	94	78
8	AIBN <sup>c</sup>	2	Air	DMC	48	88	79
9	NaNO <sub>2</sub> /Amberlyst-15	10	O <sub>2</sub>	CH <sub>2</sub> Cl <sub>2</sub> /H <sub>2</sub> O	0.5	96	80
10	MnTPPCl <sup>e</sup>	0.1	O <sub>2</sub>	C <sub>6</sub> H <sub>5</sub> CH <sub>3</sub>	2	98	81
11	CuLX <sub>2</sub>	3.7 (Cl) 3.2 (Br)	NaIO <sub>4</sub>	CH <sub>3</sub> CN/H <sub>2</sub> O	0.83	90(Cl) 85(Br)	This work

<sup>a</sup>Using visible-light as the precise driving energy; <sup>b</sup>Reaction performed at 80 °C; <sup>c</sup>Reaction performed at 60 °C; <sup>d</sup> Reaction performed at reflux condition; <sup>e</sup> Using benzaldehyde as an oxygen acceptor and temperature (50 °C); DMC: Dimethyl carbonate.

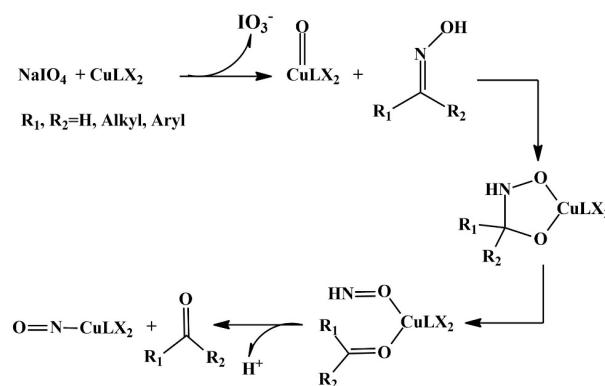
of their melting points (m.p.) and IR spectra with those of authentic samples.

The comparison of our obtained deoxygenation results with other reports (Table 3) highlights the remarkable capability of CuLX<sub>2</sub> Schiff-base complexes as oxidative catalysts. Notably, in most of reports the amount of catalyst and reaction times are higher. Also, the reactions performed in hard conditions like high temperature (entries 3, 4, 6, and 8). In case of entry 2 ((PhTe)<sub>2</sub>), visible-light used as precise driving energy.

Also, in the case of MnTPPCl (entry 10), benzaldehyde used as oxygen acceptor. In contrast, the use of CuLX<sub>2</sub> Schiff-base complexes offers several advantages can be mentioned as follows: simple working condition (stirring at room temperature), using NaIO<sub>4</sub> as a mild oxidant than H<sub>2</sub>O<sub>2</sub>, low reaction times and high product yields.

Deoxygenation mechanisms have been extensively studied and reported.<sup>81-83</sup> The expansion of mild and effective systems for the selective conversion of oxime derivatives to carbonyl compounds continues to be a substantial aspect of organic chemical transformation. Metal-mediated deoxygenation can be realized by hydrolytic, reductive, and oxidative methods.<sup>83</sup> Although mechanisms of oxidative deoxygenation depend on the reaction conditions and the type of catalyst, the general principle is that a metal center in high oxidation state (e.g., M<sup>n</sup>=O or M<sup>n-1</sup>-O•) takes two electrons, with the consequent

generation of nitroso complexes. According to using NaIO<sub>4</sub> as oxidant, the suggested mechanism of deoxygenation in the presence of CuLX<sub>2</sub> Schiff-base complexes are shown in the below scheme.

**Scheme 2.** Suggested mechanism of deoxygenation in the presence of CuLX<sub>2</sub> Schiff-base complexes

### Cytotoxic properties (*in vitro*)

Cytotoxic properties of compounds against A549 and HT29 tumor cell lines are showing in Figures 3 and 4. Figure 3 proved the studies under the microscope after 24 h exposure to the free ligand and Cu(II) complexes, the cancer cells showed characteristic cell death features in a dose-dependent manner. For the A549 cell line, we

observed chromatin and pronounced nuclear condensation. Microscopic survey revealed that normal cells maintained their natural round shape with uniform nuclei, whereas dead cells exhibited wrinkled morphology, vacuolated cytoplasm, small nuclei, and nuclear fragmentation. The treated cells displayed fragmented and condensed nuclei, characteristic of cellular shrinkage, which is a distinctive hallmark of apoptosis. For the HT29 cancer cell line, the control cells remained smooth and flat, exhibiting an even cell surface resembling that of normal healthy cells. However, as depicted in the photomicrograph, following treatment with the ligand and complexes, a pronounced alteration was observed in the cell morphology. The treated cells assumed a rounded shape, indicative of cellular shrinkage, along with vacuolated cytoplasm and small nuclei, characteristic features of cell death.

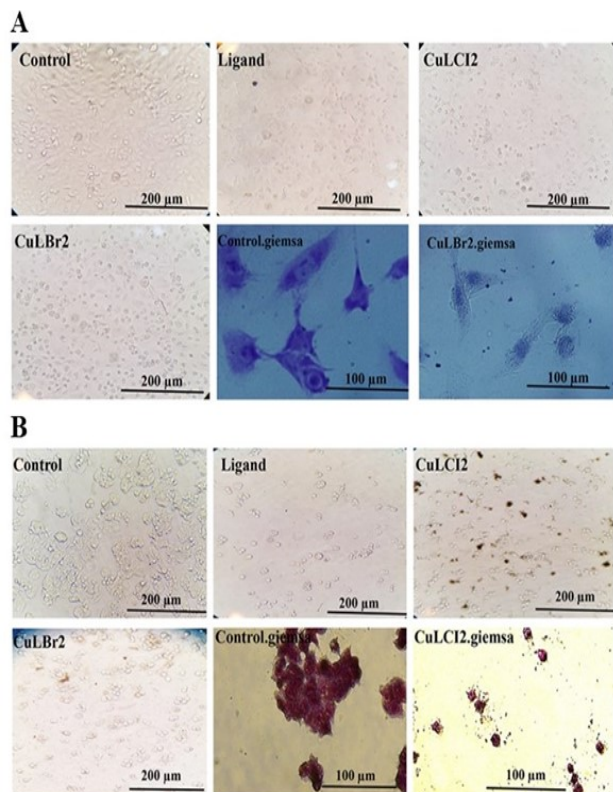


**Figure 3.** Inverted microscopic observation and Giemsa staining for a survey of cytotoxicity of ligands and Copper complexes with an  $IC_{50}$  concentration in (A) A549 and (B) HT29 cancer cell lines after 24 h.

We conducted a cytotoxicity assay, specifically the MTT assay, to assess the cell viability in the cultured cells. Based on the obtained results, by increasing the concentration of compounds on cancer cell lines, the cell growth and cell viability were decreased. Cell viability is influenced by the interplay between the cells and the culture medium. Figure 4 illustrates the outcomes of the MTT assay conducted on 24 h cell cultures, revealing

significantly higher viability in the control samples as opposed to the cells exposed to the ligand and complexes. This finding demonstrates that these components exhibit anticancer activity at the tested concentrations. In addition, our observation confirmed that copper complexes were meaningfully more efficient than ligand. Indeed, over the subsequent 72 hours, the viability of treated cells decreased compared to cells cultured in control samples and the initial day. In this study, copper complexes showed higher cytotoxic activity than its corresponding ligand. For A549 cancer cells the  $CuLBr_2$  was the most effective, while in the case of HT29 cancer cells the  $CuLCl_2$  is most effective. Totally, the data on cell viability in A549 cells suggests that, the 0.01, 0.1, and 1  $mg\ mL^{-1}$  doses of  $CuLBr_2$  (more effective compound) led to a great reduction in cell viability nearly 69%, in comparison to control after 24 h. As proved by these data, we can present these Schiff-base ligand and copper complexes as useful and efficient compounds for cancer therapy in future.

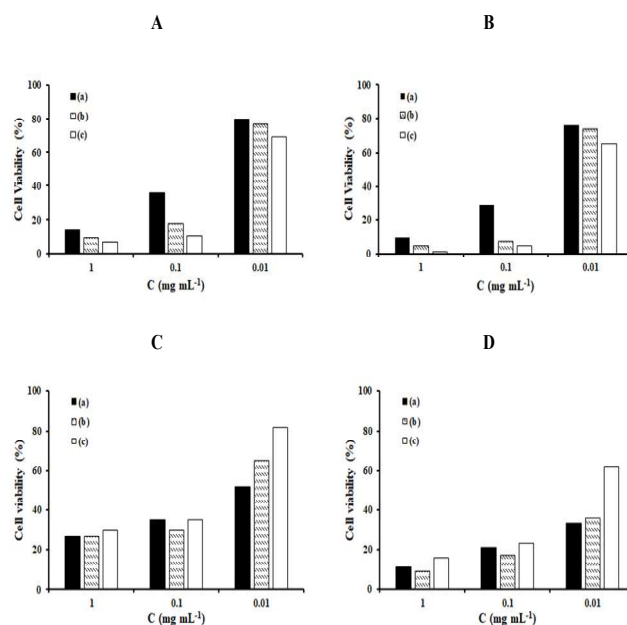


**Figure 4.** Effect of ligand and copper(II) complexes with concentrations of 0.01, 0.1 and 1  $mg\ mL^{-1}$  on cell viability of A549 (A and B) and HT29 (C and D) cancer cells: MTT assay of treated after 24 h (A and C) and 72 h (B and D) [ $p < 0.05$  and Values are mean ( $n=3$ ), Ligand (a),  $CuLCl_2$  (b) and  $CuLBr_2$  (c)].

#### 4. CONCLUSIONS

A novel asymmetric bidentate Schiff-base ligand was synthesized by condensation reaction between 4-nitro-1,2-phenylenediamine and trans-cinnamaldehyde and its complexation capacity towards  $Cu^{2+}$  has been studied. The structures of the ligand and complexes were confirmed by elemental analysis, thermal studies,  $^1H$  NMR,  $^{13}C$  NMR, FT-IR, UV-Vis spectra and molar conductance. Additionally, thermal analyses were

conducted on all compounds, ranging from room temperature to 750 °C. The results obtained from the thermal curves of both the ligand and copper complexes provided evidence that there are no water molecules present in the structures of the complexes. The electrochemical characteristics of the coordination complexes in compared to ligand was described. Copper chloride and bromide complexes exhibited different voltammograms with respect to the free ligand. Also, catalytic activities these complexes were investigated in the deoxygenation of oximes with sodium periodate. All the reactions occurred with high selectivity for carbonyl compounds formation. At last, in vitro cytotoxic efficacy of all compounds was assessed against A549 and HT29 cancer cell lines. The findings demonstrated enhanced biological activity in the complexes compared to the free ligand.

### DECLARATION OF COMPETING INTEREST

The authors declare that they have no known competing financial interests or personal relationships that could have appeared to influence the work reported in this paper.

### SUPPORTING INFORMATION

Supporting information consists of experimental sections, FT-IR, UV-Vis, <sup>1</sup>H and <sup>13</sup>C NMR spectra, TGA thermograms of ligand and Cu(II) complexes, and obtained data from solvent and catalyst amounts optimization.

### ACKNOWLEDGMENTS

Financial support for this work by the Ilam University and Shahid Chamran University of Ahvaz, are gratefully acknowledged.

### AUTHOR INFORMATION

#### Corresponding Author

Zahra Saedi: Email: [z\\_saedi@yahoo.com](mailto:z_saedi@yahoo.com), [ORCID: 0000-0001-5950-6936](https://orcid.org/0000-0001-5950-6936)

#### Author(s)

Mahmoud Roushani, Elham Hoveizi, Mohammad Hadian

### REFERENCES

1. R. Shivhare, K. Danao, D. Nandurkar, V. Rokde, A. Ingole, A. Warokar, U. Mahajan, Schiff Base in Organic, Inorganic and Physical Chemistry; Chapter 6- Schiff Base as Multifaceted Bioactive Core, IntechOpen, **2022**.
2. M. N. A. Bitu, M. S. Hossain, A. A. S. M Zahid, C. M. Zakaria, M. Kudrat-E-Zahan, *Am. J. Hetero. Chem.* **2019**, *5*, 11-23.
3. V. Xu, B. Pandey, J. P. I. D. Jayawardhena, J. A. Krause, H. Guan, *Dalton Trans.* **2023**, *52*, 11543-11551.
4. C. Boulechfar, H. Ferkous, A. Delimi, A. Djedouani, A. Kahlouche, A. Boublia, A. S. Darwish, T. Lemaoui, R. Verma, Y. Benguerba, *Inorg. Chem. Commun.* **2023**, *150*, 110451.
5. D. Iacopetta, J. Ceramella, A. Catalano, A. Mariconda, F. Giuzio, C. Saturnino, P. Longo, M. S. Sinicropi, *Inorganics* **2023**, *11*, 320.
6. E. T. B. Al-Tikrity, A. A. Yaseen, E. Yousif, D. S. Ahmed, M. H. Al-Mashhadani, *Polym. Polym. Compos.* **2022**, *30*, 1-11.
7. D. S. Ahmed, M. Kadhom, A. G. Hadi, M. Bufaroosha, N. Salih, W. H. Al-Dahhan, E. Yousif, *Chemistry* **2021**, *3*, 288-295.
8. K. Muthamma, D. Sunil, P. Shetty, S. D. Kulkarni, P. J. Anand, D. Kekuda, *Prog. Org. Coat.* **2021**, *161*, 106463.
9. H. Sun, J.-Y. Li, F.-F. Han, R. Zhang, Y. Zhao, B.-X. Miao, Z.-H. Ni, *Dyes Pigm.* **2019**, *167*, 143-150.
10. J. Ceramella, D. Iacopetta, A. Catalano, F. Cirillo, R. Lappano, M. S. Sinicropi, *Antibiotics* **2022**, *11*, 191.
11. A. Catalano, M. S. Sinicropi, D. Iacopetta, J. Ceramella, A. Mariconda, C. Rosano, E. Scali, C. Saturnino, P. Longo, *Appl. Sci.* **2021**, *11*, 6027.
12. M. N. Uddin, S. S. Ahmed, S. M. R. Alam, *J. Coord. Chem.* **2020**, *73*, 3109-3149.
13. A. Adabi Ardakani, *Inorg. Chem. Res.* **2023**, *7*, 1-6.
14. N. Aggarwal, S. Maji, *Rev. Inorg. Chem.* **2022**, *42*, 363-383.
15. B. D. Nath, M. M. Islam, M. R. Karim, S. Rahman, M. A. A. Shaikh, P. E. Georghiou, M. Menelaou, *ChemistrySelect* **2022**, *7*, e202104290.
16. A. Ali, M. Pervaiz, Z. Saeed, U. Younas, R. Bashir, S. Ullah, S. M. Bukhari, F. Ali, S. Jelani, A. Rashid, A. Adnan, *Inorg. Chem. Commun.* **2022**, *145*, 109903.
17. W. Zafar, S. H. Sumrra, Z. H. Chohan, *Eur. J. Med. Chem.* **2021**, *222*, 113602.
18. A. A. Hamed, I. A. Abdelhamid, G. R. Saad, N. A. Elkady, M. Z. Elsabee, *Int. J. Bio. Macromol.* **2020**, *153*, 492-501.
19. M. Hatefi Ardakani, A. Naeimi, *Inorg. Chem. Res.* **2022**, *6*, 176-181.
20. M. S. S. Adam, L. H. Abdel-Rahman, A. M. Abu-Dief, N. A. Hashem, *Inorg. Nano-Met. Chem.* **2020**, *50*, 136-150.
21. J. L. Pratihari, P. Mandal, C. K. Lai, S. Chattopadhyay, *Polyhedron* **2019**, *161*, 317-324.
22. J. L. Pratihari, P. Mandal, P. Brandão, D. Mal, V. Felix, *Inorganica Chim. Acta* **2018**, *479*, 221-228.
23. M. Ikram, S. Rehman, I. Feroz, Farzia, R. Khan, M. O. Sinnokrot, F. Subhan, M. Naeem, C. Schulzke, *J. Mol. Struct.* **2023**, *1278*, 134960.
24. V. Asghariazar, M. Amini, Z. Pirdel, R. Fekri, A. Asadi, K. Nejati-Koshki, B. Baradaran, Y. Panahi,

- Med. Oncol.* **2023**, *40*, 271.
25. J. Hu, Y. Luo, M. Hou, J. J. Qi, L. L. Liang, W. G. Li, *Appl. Organomet. Chem.* **2022**, *36*, e6833.
26. S. Zehra, S. Tabassum, F. Arjmand, *Drug Discov. Today* **2021**, *26*, 1086-1096.
27. H. Y. Khan, M. T. Zeyad, S. Akhter, S. Tabassum, F. Arjmand, *Inorganic Chim. Acta* **2022**, *538*, 120978.
28. H. A. Kiwaan, A. S. El-Mowafy, A. A. El-Bindry, *J. Mol. Liq.* **2021**, *326*, 115381.
29. Z. Gul, N. U. Din, E. Khan, F. Ullah, M. N. Tahir, *J. Mol. Struct.* **2020**, *1199*, 126956.
30. S. J. Kirubavathy, S. Chitra, *Mater. Today: Proc.* **2020**, *33*, 2331-2350.
31. Z. Ude, K. Kavanagh, B. Twamley, M. Pour, N. Gathergood, A. Kellett, C. J. Marmion, *Dalton Trans.* **2019**, *48*, 8578-8593.
32. V. Sumalatha, D. Ayodhya, *Results Chem.* **2023**, *5*, 100821.
33. R. Fouad, O. M. I. Adly, *J. Mol. Struct.* **2021**, *1225*, 129158.
34. Y. Cui, M. Pan, J. Ma, X. Song, W. Cao, P. Zhang, *Mol. Cell. Biochem.* **2021**, *476*, 493-506.
35. Y. Fan, L. Lin, F. Yin, Y. Zhu, M. Shen, H. Wang, L. Du, S. Mignani, J.-P. Majoral, X. Shi, *Nano Today* **2020**, *33*, 100899.
36. P. Kumar, S. Tomar, K. Kumar, S. Kumar, *Dalton Trans.* **2023**, *52*, 6961-6977.
37. U. K. Komarnicka, M. K. Lesiów, M. Witwicki, A. Bieńko, *Separations* **2022**, *9*, 73.
38. Y. Jiang, Z. Huo, X. Qi, T. Zuo, Z. Wu, *Nanomedicine* **2022**, *17*, 5.
39. S. U. parsekar, K. Paliwal, P. Haldar, P. K. S. Antharjanam, M. Kumar, *ACS Omega* **2022**, *7*, 2881-2896.
40. X. Rana, L. Wang, D. Cao, Y. Lin, J. Hao, *Appl. Organometal. Chem.* **2011**, *25*, 9-15.
41. G. G. Mohamed, M. M. Omar, A. A. Ibrahim, *Spectrochim. Acta Part A* **2010**, *75*, 678-685.
42. W. J. Geary, *Coord. Chem. Rev.* **1971**, *7*, 81-122.
43. R. Golbedaghi, A. Mohammadzaheri, M. Liyaghati-Delshad, N. Ajami, M. J. Mahdavi Lasibi, *Inorg. Chem. Res.* **2023**, *7*, 22-26.
44. H. Kargar, M. Fallah-Mehrjardi, R. Behjatmanesh-Ardakani, K. S. Munawar, *Inorg. Chem. Res.* **2022**, *6*, 48-57.
45. V. Mirdarvatan, B. Bahramian, A. Dehno Khalaji, S. J. Peyghoun, M. Dusek, V. Eigner, *Inorg. Chem. Res.* **2021**, *5*, 10-18.
46. H. Temel, S. İlhan, M. Şekerci, *Synth. React. Inorg. Met.-Org. Chem.* **2002**, *32*, 1625-1634.
47. A. A. Mohamed, A. A. Nassr, S. A. Sadeek, N. G. Rashid, S. M. Abd El-Hamid, *Compounds* **2023**, *3*, 376-389.
48. P. Deivanayagam, R. Pa. Bhoopathy, S. Thanikaikarasan, *Int. J. Adv. Chem.* **2014**, *2*, 166-170.
49. L. P. Nitha, R. Aswathy, N. E. Mathews, K. Mohanan, *Spectrochim. Acta Part A* **2014**, *118*, 154-161.
50. Y. Harinath, D. H. Kumar Reddy, B. N. Kumar, Ch. Apparao, K. Sessaiah, *Spectrochim. Acta Part A* **2013**, *101*, 264-272.
51. G. H. Grivani, V. Tahmasebi, K. Eskandari, A. K. Dehno Khalaji, G. Bruno, H. Amiri Rudbari, *J. Mol. Struct.* **2013**, *1054*, 100-106.
52. A. Y. Obali, H. I. Ucan, *J. Fluoresc.* **2016**, *26*, 1685-1697.
53. M. S. Refat, I. M. El-Deen, H. K. Ibrahim, S. El-Ghool, *Spectrochim. Acta Part A* **2006**, *65*, 1208-1220.
54. E. I. Solomon; A. B. P. Lever, *Inorganic Electronic Structure and Spectroscopy, Volume II: Applications and Case Studies*, Wiley, New York, **1999**.
55. R. Arab Ahmadi, S. Amani, *Molecules* **2012**, *17*, 6434-6448.
56. S. Amani, G. A. van Albada, J. Reedijk, *Transit. Metal Chem.* **1999**, *24*, 104-107.
57. C. Sino, S. A. Holt, *Inorg. Chem.* **1968**, *7*, 2655-2657.
58. M. Montazerzohori, S. Farokhiyani, A. Masoudiasl, J. M. White, *RSC Adv.* **2016**, *6*, 23866-23878.
59. M. Montazerzohori, A. Nazaripour, A. Masoudiasl, R. Naghiha, M. Dusek, M. Kucerakova, *Mater. Sci. Eng. C* **2015**, *55*, 462-470.
60. M. Amirnasr, K. J. Schenk, M. Salavati, S. Dehghanpour, A. Taeb, A. Tadjarodi, *J. Coord. Chem.* **2003**, *56*, 231-243.
61. A. H. Kianfar, M. Paliz, M. Roushani, M. Shamsipur, *Spectrochim. Acta Part A* **2011**, *82*, 44-48.
62. A. H. Kianfar, V. Sobhani, M. Dostani, M. Shamsipur, M. Roushani, *Inorg. Chim. Acta* **2011**, *365*, 108-112.
63. S. Bollo, L. J. Núñez-Vergara, C. Barrientos, J. A. Squella, *Electroanalysis* **2005**, *17*, 1665-1673.
64. J. A. Squella, P. Gonzalez, S. Bollo, L. J. Núñez-Vergara, *Pharm. Res.* **1999**, *16*, 161-164.
65. A. Khoshdast, S. A. Beyramabadi, S. Allameh, Maryam Hashi, A. Morsali, M. Pordel, *Inorg. Chem. Res.* **2022**, *6*, 26-30.
66. Z. Ghamati, M. Pordel, A. Davoodnia, S. A. Beyramabadi, *Inorg. Chem. Res.* **2022**, *6*, 69-75.
67. H. Kargar, M. Fallah-Mehrjardi, R. Behjatmanesh-Ardakani, K. S. Munawar, M. Bahadori, M. Moghadam, *Inorg. Chem. Res.* **2022**, *6*, 76-83.
68. H. Kargar, M. Fallah-Mehrjardi, *Inorg. Chem. Res.* **2021**, *5*, 201-206.
69. M. Sutradhar, E. C. B. A. Alegria, T. R. Barman, H. M. Lapa, M. F. C. G. da Silva, A. J. L. Pombeiro, *Inorganica Chim. Acta* **2021**, *520*, 120314.
70. O. Santoro, X. Zhang, C. Redshaw, *Catalysts* **2020**, *10*, 800.
71. M. Sutradhar, T. R. Barman, E. C. B. A. Alegria, H. M. Lapa, M. F. C. G. da Silva, A. J. L. Pombeiro, *New J. Chem.* **2020**, *44*, 9163-9171.



72. N. Vijayakumari, B. Balakrishna Reddy, L. Nagarapu, *Heterocycl. Commun.* **2006**, *12*, 407-410.
73. X. Denga, R. Qian, H. Zhou, L. Yu, *Chin. Chem. Lett.* **2021**, *32*, 1029-1032.
74. W. Li, F. Wang, Y. Shi, L. Yu, *Chin. Chem. Lett.* **2023**, *34*, 107505.
75. X. Deng, H. Cao, C. Chen, H. Zhou, L. Yu, *Sci. Bull.* **2019**, *64*, 1280-1284.
76. P. J. Das, A. Das, A. Baruah, *Indian J. Chem.* **2010**, *49B*, 1140-1143.
77. X. Jing, D. Yuan, L. Yu, *Adv. Synth. Catal.* **2017**, *359*, 1194-1201.
78. Y. Li, N. Xu, G. Mei, Y. Zhao, Y. Zhao, J. Lyu, G. Zhang, C. Ding, *Can. J. Chem.* **2018**, *96*, 810-814.
79. F. Wang, T. Chen, Y. Shi, L. Yu, *Asian J. Org. Chem.* **2021**, *10*, 614-618.
80. G. Zhang, X. Wen, Y. Wang, W. Mo, C. Ding, *J. Org. Chem.* **2011**, *76*, 4665-4668.
81. X. -T. Zhou, Q. -L. Yuan, H. -B. Ji, *Tetrahedron Lett.* **2010**, *51*, 613-617.
82. Y. Zheng, A. Wu, Y. Ke, H. Cao, L. Yu, *Chin. Chem. Lett.* **2019**, *30*, 937-941.
83. D. S. Bolotin, N. A. Bokach, M. Y. Demakova, V. Y. Kukushkin, *Chem. Rev.* **2017**, *117*, 13039-13122.